Gas-phase photolytic production of hydroxyl radicals in an ultraviolet purifier for air and surfaces

David R. Crosley, Connie J. Araps, Melanie Doyle-Eisele & Jacob D. McDonald

Taylor & Francis
Taylor & Francis Group

TECHNICAL PAPER

∂ OPEN ACCESS

Gas-phase photolytic production of hydroxyl radicals in an ultraviolet purifier for air and surfaces

David R. Crosley[a], Connie J. Araps[b], Melanie Doyle-Eisele[c], and Jacob D. McDonald[c]

[a]Private consultant to HGI Industries (Boynton Beach, Florida), Palo Alto, CA, USA; [b]Prometheus Strategies, Delray Beach, FL, USA; [c]Lovelace Respiratory Research Institute, Albuquerque, NM, USA

ABSTRACT

We have measured the concentration of hydroxyl radicals (OH) produced in the gas phase by a commercially available purifier for air and surfaces, using the time rate of decay of *n*-heptane added to an environmental chamber. The hydroxyl generator, an Odorox® BOSS™ model, produces the OH through 185-nm photolysis of ambient water vapor. The steady-state concentration of OH produced in the 120 m^3 chamber is, with 2σ error bars, $(3.25 \pm 0.80) \times 10^6$ cm^{-3}. The properties of the hydroxyl generator, in particular the output of the ultraviolet lamps and the air throughput, together with an estimation of the water concentration, were used to predict the amount of OH produced by the device, with no fitted parameters. To relate this calculation to a steady-state concentration, we must estimate the OH loss rate within the chamber owing to reaction with the *n*-heptane and the 7 ppb of background hydrocarbons that are present. The result is a predicted steady-state concentration in excellent agreement with the measured value. This shows we understand well the processes occurring in the gas phase during operation of this hydroxyl radical purifier.

Implications: Hydroxyl radical air purifiers are used for cleaning both gaseous contaminants, such as volatile organic compounds (VOCs) or hazardous gases, and biological pathogens, both airborne and on surfaces. This is the first chemical kinetic study of such a purifier that creates gas-phase OH by ultraviolet light photolysis of H_2O. It shows that the amount of hydroxyls produced agrees well with nonparameterized calculations using the purifier lamp output and device airflow. These results can be used for designing appropriate remediation strategies.

Introduction

The hydroxyl radical, OH, is present throughout the troposphere (Crosley, 1995; Stone et al., 2012). The steady-state concentration is very much less than a part per trillion; typical concentrations outdoors on a sunny day are 3×10^6 molecules/cm^3. Even at these low concentrations, OH is the primary oxidant for nearly all source gases emitted into the troposphere, be they manmade, such as many nonmethane hydrocarbons and halogenated hydrocarbons, or natural, such as isoprenes and terpenes. This is due to to its very high reactivity removing any labile hydrogens and its ability to add into double and triple bonds. For many compounds, the reaction rate coefficients are close to gas kinetic, occurring on nearly every collision.

In the troposphere, the hydroxyl radical's major mode of formation follows the photolysis of O_3 by sunlight in the spectral region having wavelengths longer than ~315 nm (shorter ultraviolet wavelengths are filtered out by the stratospheric ozone layer). This

forms excited $O(^1D)$ atoms, some of which then react with H_2O, also naturally present, to form two OH radicals. (About 90% of the $O(^1D)$ are quenched by atmospheric gases to the $O(^3P)$ ground state, which reforms an O_3 through reaction with O_2.)

The loss of OH is due overwhelmingly to reaction by the gases it oxidizes. In the remote troposphere, its chemical lifetime ranges from a few tenths of a second up to about 1 sec. In highly polluted regions, it can be considerably less. Because of its short lifetime, knowledge of the OH concentration forms a most valuable test of the chemistry of the troposphere, as it is not directly affected by surface sources and sinks: only those source gas concentrations in a limited spatial region, and not time histories of an air parcel, determine the local OH concentration.

This natural atmospheric cleansing phenomenon can be turned to a technologically advantageous method for the removal of a large variety of noxious, hazardous, or simply unwanted compounds produced in an enclosed

area such as a room or workspace. Several commercially available apparatus have been developed for this purpose in the last several years. All of these involve some sort of direct or indirect photolytic formation of OH radicals, either in the gas phase or on catalytic surfaces. These formation processes are the photolysis of O_3 as in the atmosphere (Johnson et al., 2014), direct photolysis of H_2O farther into the ultraviolet as presented here, or the OH formed as the result of a photolytically generated electron–hole pair on a catalytic surface, usually TiO_2 (Mo et al., 2009).

The gas-phase photolytic methods can generally be scaled using multiple light sources to treat a variety of sizes of commercial spaces, from a thousand to several million cubic feet, as the amount of OH generated is proportional to the amount of incident ultraviolet radiation. In contrast, the catalytic method is usually used to treat smaller spaces as the amount of OH reacting is limited by the surface area of the catalyst and rate of adsorption of the reactants onto the surface.

Indoor air is usually far more heavily polluted than outdoors (Weschler, 2009), and often contains health hazards that need to be removed, such as volatile organic chemicals and airborne microorganisms such as bacteria, viruses, or mold. In other situations persistent pollutants, such as lingering odors from a fire, cigarette smoke, or cooking, may hamper the use of indoor spaces. When sufficient concentrations of free (i.e., not surface-bound) OH are generated indoors—similar to those found in nature—microorganisms and even mold can be decomposed and neutralized in air and on surfaces (Steinagel, 2009; Ramm, 2009). Therefore, the use of these methods has found widespread use in many situations and applications.

Nonetheless, despite reasonable purported mechanisms for the generation of OH and its oxidation of the various target compounds, only quite recently has there been performed any direct chemical kinetic investigation showing the existence of OH radicals (Johnson et al., 2014). In that work, the OH was formed following the generation of O_3 and its photolysis at 254 nm, in a system designed to react away hydrocarbons in a sequence that ends in fine particulates that are then removed by electrostatic precipitation. Other tests using the photocatalytically generated method (Mo et al., 2009) do show removal of target compounds but not in a quantitative way allowing any mechanistic information to be derived.

Here, we show quantitatively that one commercial device, which generates OH entirely in the gas phase by the direct photolysis of ambient H_2O vapor at 185 nm, oxidizes a hydrocarbon (*n*-heptane) in a test chamber designed for chemical kinetic studies. We use the rate of removal of the *n*-heptane to derive an effective gas-phase concentration of OH. This is then compared with predictions obtained from a quantitative theoretical treatment of the device's photolytic production rate together with an estimate of the loss rate for OH due to the *n*-heptane and background hydrocarbons.

The experiment

The generation of OH radicals

The experiment was conducted using a particular air purifier, operating entirely in the gas phase, relying on the photolysis of ambient H_2O vapor using 185-nm radiation from mercury lamps to produce the hydroxyl radicals. The particular purifier studied was an Odorox® BOSS™ model. Designed to treat 4000 to 16,000 cubic feet—an average-sized commercial space—it has two lamps with an output of ~40 W total, and a throughput rate of 400 cfm (190 liters/sec) in these experiments. For the purposes of understanding the experiments, the hydroxyl generator may be considered simply to be a small box of 3.28 L internal active volume containing the lamps, with the outside air passing continuously through, via a fan that is part of the purifier apparatus.

The lamps produce radiation at 185 and 254 nm; light produced at any other wavelength is not relevant to hydroxyl production. Although the 254-nm radiation could photolyze ozone to produce OH, this process may be ignored in this apparatus, as shown later. For OH, the pertinent photolysis reactions at 185 nm are:

$$H_2O + h\nu_{185} \rightarrow H + OH \qquad (1)$$

$$H + O_2 + M \rightarrow HO_2 + M \qquad (2)$$
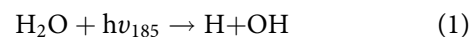
and soon after, the hydroperoxyl radical HO_2 is converted to a hydroxyl:

$$HO_2 + NO \rightarrow OH + NO_2 \qquad (3)$$

or sometimes

$$HO_2 + O_3 \rightarrow OH + 2O_2 \qquad (4)$$
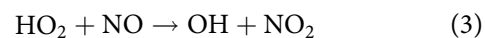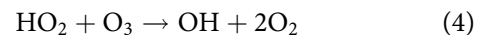
where the NO or ozone is present in the local environment, and $h\nu_{185}$ denotes a photon at 185 nm. Thus two OH radicals are formed for each H_2O molecule initially photolyzed.

At the same time, O_3 is formed from the photolysis of O_2 by the same radiation:

$$O_2 + h\nu_{185} \rightarrow O + O \qquad (5)$$

$$O + O_2 + M \rightarrow O_3 + M \qquad (6)$$
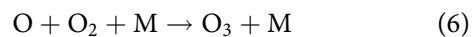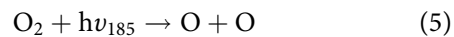
so that, as with OH from water, two ozone molecules are produced for each O_2 photolyzed. The ozone that is

produced is inconsequential with regard to the operation or function of the purifier as studied in the experiment described in this paper, although it does form a very useful quantitative test of the operation of the device (see later discussion).

The M in the preceding reactions is a third ambient molecule, either O_2 or N_2. Such a "three-body reaction" is necessary to remove the excess energy produced when the H or O atom reacts with O_2; otherwise, the two reactants would have so much energy they would just fly apart again without reacting. Despite the necessity for three entities to collide at once, these processes are quite fast (Logan et al., 1981), occurring within 30 nsec for H and 3μsec for O. We consider quantitative details of these processes in the following, in the discussion of the calculation of the production of OH radicals by the device.

The chemical kinetics measurements

The measurements, conducted at the Lovelace Respiratory Research Institute in Albuquerque, NM, are performed in an environmental chamber of 120 m³, or 120,000 L. The interior surfaces are made of inert "water-clear" Teflon film to eliminate wall reactions. The chamber is purged with background air drawn through a HEPA filter. Gas chromatography/mass spectrometry measures background compounds; these do not interfere with the measurements themselves but must be considered in the analysis of OH loss rates. For all experiments, the OH generator was placed in the middle of the chamber, with an extension cord passing through a small hole in the floor to permit remote operation. The chamber contained two mixing fans, one at each end, to assure complete mixing of the gases within.

A slow flow of outside (filtered) air continually enters the chamber, and exits through the instrument sampling ports, so that a constant small dilution of all gases within occurs; this must be accounted for in the analysis of the decay of the hydrocarbon concentration. To monitor this, all experiments were conducted with the addition of a low concentration of a nonreactive tracer, CCl_4. Typically the chamber contents are diluted between 1 and 3% per hour over a series of several experiments; in the experiment discussed here, the rate was 1.50% per hour. This necessary correction can be applied before the analysis, or, as done in the case of these n-heptane measurements, as part of the data analysis procedure itself. Although other species were sometimes monitored, the pertinent ones for the present experiment are the O_3 and the n-heptane. The former is measured using a standard commercial absorption instrument operating at 254 nm, and the hydrocarbon via the gas chromatography/mass spectrometry instrument. These measurements are made on air continuously sampled through small ports in the chamber itself.

The ozone measurements are determined by the instrument as a fractional concentration, parts per billion. However, that is not meaningful in itself as a measure of the production rate of the compound by the hydroxyl generator, as the ozone is here generated in a closed chamber with neither gas phase nor wall losses (see later discussion). The meaningful quantity is the production in absolute amount per hour, which will be used below as one metric of the performance of the device. For the April run discussed in detail in the following, we find the O_3 to be produced at the rate of 0.041 g/hr.

The decay measurements of n-heptane were conducted typically for about 2 hr after the device was turned on, with nonoperating stabilization periods of an hour or more both before and after, during which measurements were also made. Three runs were made. Two of these were in April, with initial concentrations of 1.36 ppm and 131 ppb of n-heptane seeded into the chamber. A third was done in October, with 135 ppb initial concentration. The 1.36 ppm run showed no decay; both of those at the lower concentration did exhibit an n-heptane loss. However, the data set for the April run at 131 ppb was far more extensive than that in October, and is thus chosen for detailed analysis. The analysis shows that the results from the other two runs are fully compatible with those from this more extensive and thoroughly analyzed experiment.

Figure 1 shows the n-heptane concentrations as a function of time. (The three straight-line fits to the data are included to guide the eye to the differences in decay rates with the device on and off, but the fit showing the reactive decay is not used for the kinetic analysis.) As expected, an initial small decay is seen, owing to the dilution; a significantly faster one during operation of the hydroxyl generator; and finally a return to the slow decay after the device is turned off.

The other important quantities are the hydrocarbons in the inlet air, measured as a group at 7 ppb but with no speciation. For understanding the rate of production of hydroxyls, we also require the ambient H_2O concentration. The temperature during the experiment is measured (21°C), but unfortunately the relative humidity (dew point) was not for this particular run. We are thus able to predict with certainty only an upper rate for the photolytic production of hydroxyl in the device, although we can make a reasonable estimate of the humidity based on average meteorological data to obtain a better result.
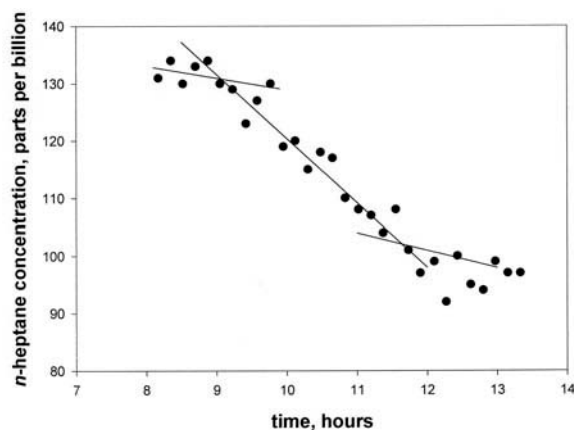
Figure 1. *n*-Heptane concentration data as a function of time. The lines are linear fits to the three different portions of the experiment: before, during, and after operation of the hydroxyl generator, as described in the text. They are meant to guide the eye to the differences in decay rates with the purifier on and off. The fit for the time the purifier is on is not used for the data analysis; see Figure 2 for the logarithmic fit. There are additional data past the right-hand side of the graph, not shown, that contribute to the fit given.

Data analysis

The decrease in the concentration of *n*-heptane is caused both by reaction with OH and by the constant dilution. With a dilution rate of b ppb/sec, the time derivative can be written

$$d[n - hep]/dt = -k[OH]_{ss}[n - hep] - b \quad (7)$$

where [n-hep] is the instantaneous *n*-heptane concentration and k is the reaction rate coefficient (Finlayson-Pitts and Pitts, 2000) for the reaction between OH and *n*-heptane, which at 300 K is equal to 7×10^{-12} cm^3 sec^{-1}. $[OH]_{ss}$ is the local steady-state concentration of OH, that is, the time-independent balance between the constant production rate, via photolysis of water, and the loss rate, due to reaction with the various gases in the chamber, including the *n*-heptane. The value of $[OH]_{ss}$ probably increases slightly throughout the experiment, but this may be ignored for the determination of an average value as done here.

It is important to consider how the steady-state approximation is used in this analysis. We show later that in actuality about half the hydroxyl radicals produced inside the purifier device do not exit. However, most of the HO$_2$ radicals do exit, and are rapidly converted to OH via reaction (3) or (4), just outside the device. However, all of those hydroxyl radicals react quickly in turn before dispersing more than a few millimeters through the chamber. Therefore, all the reactions with *n*-heptane (and any other background gases) occur quite close to the location where the OH

and HO$_2$ are produced. Nonetheless, despite reacting only within or very close to the device, the *n*-heptane is mixed uniformly throughout the chamber much more quickly than its concentration decreases. It is this average concentration that is sampled and measured in order to determine the amount of OH present.

Because the average hydrocarbon concentration is measured, it is useful to envision the entire chemical sequence as due to the continuous local production of OH, evenly distributed throughout the entire chamber, with the radicals quickly reacting, instantaneously attaining a steady-state concentration balance at $[OH]_{ss}$ and removing the *n*-heptane. This is usually referred to as a well-stirred reactor model and serves well for the analysis purpose here.

Equation (7) is easily integrated to obtain

$$\ln\{(a[n - hep]_0 + b)/(a[n - hep]_1 + b)\} = k[OH]_{ss}\Delta t, \quad (8)$$

where $[n-hep]_t$ is the concentration of the hydrocarbon at time t, Δt is the time difference $t_1 - t_0$, and a is the product $k[OH]_{ss}$. A logarithmic plot of the data obtained while the device is operating is shown in Figure 2. To solve this equation for the steady-state concentration of OH, we must first estimate b/a, and then iterate.

Details of the analysis are given in the supporting information (SI). The iteration converges quickly to $(3.25 \pm 0.80) \times 10^6$ cm^{-3}, as averaged throughout the entire test chamber. The 2σ error bars arise from the fit shown in Figure 2.

The October run was fit as linear decays for comparison with the April run, and the result is compatible: $(4.5 \pm 2.6) \times 10^6$ cm^{-3}. For this particular run, the
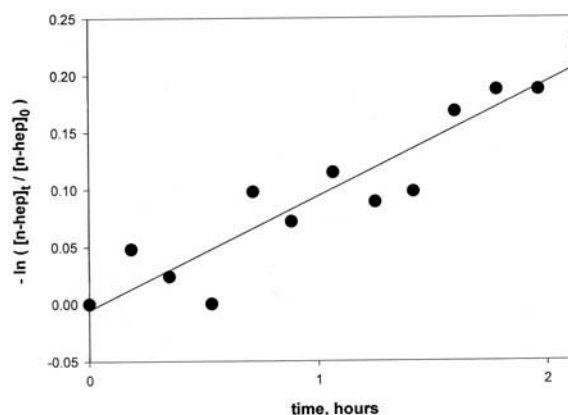

Figure 2. Logarithmic plot of the *n*-heptane concentration during operation of the hydroxyl generator. It is turned on at *t* = 0, the left-hand side of the plot, and off at *t* = 2.1 hr, the right-hand side.

temperature and dew point were recorded, so the water concentration is known.

One run was made in April, at a 10-fold higher concentration of *n*-heptane, showing a net loss of (5.5 ± 49) ppb/hr, that is, no significant change. Here, the production rate of OH in the hydroxyl generator is the same as in the other runs, but its loss rate is more than six times larger, caused by the higher *n*-heptane concentration, thus producing a steady-state concentration that will be sixfold smaller. Thus, the fractional *n*-heptane loss is six times less, and was obscured by the dilution and noise in the data.

The results for the three runs, together with predicted OH concentrations calculated as described in the next section, are given in Table 1.

Calculated rate of production of hydroxyl radicals

The rate of production of OH is calculated from knowledge of the output of the lamps used in the purifier together with the ambient atmospheric conditions. We begin with reactions (1)–(4); reaction (3) follows in ~0.1 to 1 sec later, depending on the [NO], and reaction (4) within a couple of minutes depending on the [O$_3$]. For the current purpose, we consider this conversion of HO$_2$ to OH as instantaneous, introducing no error.

We write the rate of formation of OH radicals, in molecules per cubic centimeter per second, as

$$d[OH]/dt = 2I_{185}\sigma_{H2O}[H_2O] \qquad (9)$$

The value 2 arises because two OH radicals are formed for each H$_2$O photolyzed. I$_{185}$ is the intensity (in photons/cm^2/sec incident on each 1 cm^3 of the experimental chamber), σ$_{H2O}$ the cross section (in cm^2) for absorption by water at 185 nm, and [H$_2$O] is the water concentration in molecules per cubic centimeter.

There are two lamps in the particular model of purifier used in this experiment, each a low-pressure Hg lamp whose output at 254 nm has been measured at HGI to be 160 μW/cm^2 at a distance of 1 m (M.E. Mino, HGI Industries, Boynton Beach, FL, private communication). This integrates to a total output

power at this wavelength of 20.1 W per lamp. A spectrum of the lamp shows that the intensity ratio in photons per second at 185 nm is 0.1 of this (B. Puente, Light Sources, Orange, CT, private communication). Twenty-one percent of the length of each lamp is constructed of a grade of quartz that passes 185 nm radiation. The measured total energy, the intensity ratio, and transmission show a total output at 185 nm of 1.07 × 10^{18} photons/sec.

The term σ$_{H2O}$ is taken from Creasey et al. (2000), who discuss their own measurements and those of others to select the best value to calibrate their laser induced fluorescence measurements of atmospheric OH (Creasey et al., 1997; Stone et al., 2012). From these we select 7.22 × 10^{-20} cm^2. Creasey et al. (2000) assign an error of about 3% to their result, which is negligible compared to other uncertainties in the following calculation.

The value of [H$_2$O] is problematic; the dew point was not measured. We use the value for 100% relative humidity (RH) at the experimental temperature of 21°C, that is, 18.65 torr [H$_2$O]. The actual water present is of course less; lack of this value is the main source of uncertainty when comparing calculation with experiment.

We visualize the photolysis reaction occurring in a cube 1 cm on a side. As in the data analysis, it is convenient to consider all the processes as distributed evenly throughout the 1.2 × 10^8 cm^3 environmental chamber. Thus, there are 8.9 × 10^9 of the 185-nm photons incident per second onto each 1 cm^3. We envision them falling on a 1-cm^2 side and passing through the 1-cm path length of this cube. Then the fraction absorbed (in this 1-cm path) will be σ$_{H2O}$[H$_2$O]; for the value [H$_2$O] = 5.97 × 10^{17}cm^{-3} appropriate for 21°C and 100% RH, this is 0.043. This corresponds to a hydroxyl production rate of 7.67 × 10^8 cm^{-3} sec^{-1}. Summing through the entire volume, we find that the device produces a total of 9.2 × 10^{16} OH molecules per second, at this (necessarily assumed) value of 100% humidity.

Similarly, we calculate the expected ozone production rate:

$$d[O_3]/dt = 2I_{185}\sigma_{O2}[O_2] \qquad (10)$$

The term σ$_{O2}$ is also taken from Creasey et al. (2000), choosing a value 1.2 × 10^{-20} cm^2. The apparent value depends on both the oxygen path length and lamp operating parameters, owing to considerable rotational structure in the Schumann–Runge band system in this wavelength region (Yoshino et al., 1984). We rather arbitrarily assign an uncertainty of 0.2 × 10^{-20} cm^2 from an examination of the figures in Creasey et al.

Table 1. Data and results for the *n*-heptane oxidation experiments.

Run date	[n-hep]0, ppb	[H2O], torr	Measured [OH]ss, 10^6/cm^3	Predicted [OH]ss, 10^6/cm^3
April	1360	—	1.8 ± 16	0.5[a]
April	131	2.80[b]	3.25 ± 0.80	2.8
October	135	9.64	4.5 ± 2.6	10

[a]Assuming 2.8 torr H$_2$O as in the other April run.
[b]Assuming 15% RH.

This constitutes the uncertainty in the calculated value of the ozone production rate.

On the other hand, $[O_2]$ is well known, with no associated uncertainty. Thus, the device should produce ozone at a total rate $(1.34 \pm 0.22) \times 10^{17}$ molecules per second. Note that this is only about 1.5 times the calculated OH production rate, whereas OH is a far stronger oxidizer than ozone, typically reacting some million times faster with most organic chemicals (Finlayson-Pitts and Pitts, 2000).

In fact, it is easy to see from eqs (9) and (10) that the ratio of OH and ozone production is independent of light intensity. The production rate ratio depends, in addition to the known cross-section ratio, only upon the variable $[H_2O]$, that is, the temperature and RH. This is true for any device producing OH solely via 185-nm photolysis. For example, for 20°C and 50% RH, 0.2 molecules of OH will be produced for each molecule of O_3, whereas for 30°C and 100% humidity the ratio is 0.7.

We later show that this experiment is probably conducted in a rather dry environment. In such a case, the OH production could be increased by adding water via a mister; such an enhancement was suggested in a patent for the device studied here (Morneault, 2010).

Discussion

Loss rates for OH and O_3

The measured quantity in the case of OH is the steady-state concentration; that for O_3 is the direct rate of production. For comparison with the predicted values in the preceding section, we need to know the rates of loss of each species. That is, $[OH]_{ss}$ is the direct balance between production rate **P** and loss rate **L**:

$$[OH]_{ss} = P/L, \qquad (11)$$

The loss of OH in the closed environment is caused by reaction with the *n*-heptane and any background hydrocarbons. The first contribution is straightforward but the latter pose somewhat of a problem, as we know their concentration but not speciation. Weschler and Shields (1996) have discussed typical hydrocarbon concentrations in indoor air, and we assume the makeup of our hydrocarbons is the same. We find (see SI) that OH is removed at a rate 41.7 sec^{-1}, that is, a chemical lifetime of 24 msec.

In the case of ozone, the loss processes are negligible. We see from the SI that in this coated, closed chamber with no source gases entering, there is neither reactive nor surface loss. We note in passing that this situation is quite different from the real-world case when some location is being cleansed. Then ozone is removed by

normal air exchange; by continually replenished source gases such as NO and organic compounds, particularly alkenes like isoprenes and terpenes; and by reactions and adsorption on surfaces. All of these loss mechanisms provide a constant removal rate from the beginning of the purifier operation, so that the ozone does not build up and never exceeds safe levels. That contrasts with the experiment discussed here, conducted in a loss-free closed environmental chamber.

Comparison of predictions and experiment

We use these **P** and **L** values, 7.67×10^8 cm^{-3} sec^{-1} and 41.7 sec^{-1}, to predict the steady-state concentration averaged throughout the entire 120,000 L chamber. This is $[OH]_{ss} = 1.84 \times 10^7$ cm^{-3}, some 5.7 times the measured value of $(3.25 \pm 0.80) \times 10^6$ cm^{-3}.

This discrepancy may be accounted for by the fact that 100% RH was used to arrive at an upper limit for $[OH]_{ss}$. However, in the afternoon and early evening in Albuquerque, NM, in April (the time of the experiment), the average humidity (Weatherspark, 2015) is about 15%. The use of this more realistic value brings the predicted steady state concentration to 2.8×10^6 cm^{-3}, which is well within the measured value and its error bars, although of course the true humidity is not known.

The other estimated variable is the loss rate **L**. The minimum owes to the *n*-heptane alone, while the maximum would occur if all 7 ppb of the hydrocarbons reacted with OH with extremely high (although realistic) reaction rate coefficients of 2×10^{-10} cm^3 sec^{-1}. The result is a possible threefold range; use of the Weschler and Shields (1996) mix happened to give a result at the average.

In October, T = 20°C with a 10.8°C dew point, yielding a pressure of 11.0 Torr H_2O, and we predict **P** = 4×10^8 cm^{-3} sec^{-1}. With the same **L** we expect $[OH]_{ss} = 1 \times 10^7$ cm^{-3}, about twice the measured value of $(4.5 \pm 2.6) \times 10^6$ cm^{-3}.

Despite the necessary assumption concerning the RH in the April experiment, there are no adjustable or fitted parameters anywhere in these calculations of predicted $[OH]_{ss}$ values. Therefore, we consider the agreement to be excellent, indicating we understand well the formation process of OH in this purifing device.

The comparison of ozone provides an independent test. This is quite straightforward, as there is no loss. Our predicted value of $(1.34 \pm 0.22) \times 10^{17}$ molecules per second corresponds to (0.0385 ± 0.0063) g/hr where the uncertainty arises from our value assigned to σ_{O2}. The experimental value was 0.041 g/hr, in excellent

agreement. Again, this shows that we understand well the fundamental operation, in particular, the action of the ultraviolet lamps.

Mode of operation of the hydroxyl generator

We now consider the spatial and temporal behavior of the hydroxyl radicals generated by this cleansing device. This is first discussed for the situation appropriate to the experiment performed here. We again stress that this differs from the real-world situation in that it is performed in a closed environment without significant air exchange which would maintain a constant concentration of source gases such as nitric oxides and organic compounds. (The only air exchange in this experiment is the 1.5% dilution, too small to affect the gas concentrations here.) These differences are discussed at the end of this subsection.

For the purposes of this discussion, the hydroxyl generator is pictured as a box 3.28 L in volume with a constant flood of 185-nm photons as discussed earlier. Water is photolyzed only within. The device's fan (not a physical part of our conceptual picture) furnishes a throughput of 400 cfm, so that the residence time of any molecule within the device is 17 msec, and the entire 120 m^3 volume of the environmental chamber passes through the purifier 5.7 times per hour. This volume of air exits through a 6" × 3" (116 cm^2) opening, so that the Reynolds number at the exit is 1.2×10^5. Thus, there is turbulent flow and mixing at the exit port, but not far beyond. This fact will be important for understanding the chemical basis of the cleansing operation.

The photolyzed water produces OH radicals and H atoms inside the device; the latter convert instantaneously (compared to any flow velocities) to HO_2 radicals. The loss rate of 41.7 sec^{-1} corresponds to a chemical lifetime of 24 msec, so that about half the hydroxyls undergo reaction within the device and about half make it to the exit port.

The hydroperoxyl radicals are converted back to OH in our experiment by O_3. In the inlet air, background ozone was present at a concentration of 52 ppb. This will (i) ensure that there is no NO present to convert the HO_2 via reaction (3) (this NO removal is discussed in the SI when considering O_3 loss rates) and (ii) convert the HO_2 itself via reaction (4). At 52 ppb ozone, this conversion will occur with a chemical lifetime of about 2 min, so that nearly all of the HO_2 exit the device and are converted to OH outside it.

Although detailed turbulent flow simulations would be necessary to specify precisely the spatial distribution of these hydroperoxyl radicals, such flow subsides near enough to the device exit port that they will remain relatively close to the hydroxyl generator, compared to the overall chamber dimensions. The diffusion coefficient for OH or HO_2 in air is about 0.2 cm^2 sec^{-1}, and the distance diffused in a time t is $(2Dt)^{1/2}$, so that after the turbulence has abated, the radicals will diffuse ~0.6 cm from their production point in one second, and ~7 cm in 2 min. The OH will have reacted long before these times, but the hydroperoxyl radicals can diffuse around the exit port for a few centimeters before conversion to OH in this experiment.

Thus, in actuality the *n*-heptane reacts with OH only within or quite near to the device itself. Inside, the true OH steady-state concentration is much higher than the average chamber value that we calculated with the well-stirred reactor model (although these averaged calculations remain valid for the purposes of the preceding sections). Within the device [OH] is 1.2×10^{11} cm^{-3} so that any *n*-heptane entering the device will react with about a 1-sec lifetime. However, recall that the *n*-heptane residence time inside the device, where the OH concentration is high, is that of any air parcel flowing through, that is, 17 msec. Therefore, on each pass through the hydroxyl generator, some 1.5% of the *n*-heptane is removed; because any air parcel passes through 5.6 times per hour, some 10% is removed per hour, in accord with observations.

In our experiment in a closed chamber, about half of the hydroxyl radicals exit; almost all the HO_2 radicals have exited the chamber and form OH a few centimeters outside the device. This is because the conversion from HO_2 to OH is here caused by O_3. In a real-world situation, there would be enough NO present to convert it much faster. The rate coefficient (DeMore et al., 1997) for the reaction $HO_2 + NO \rightarrow OH + NO_2$ at 300 K is 8.1×10^{-12} cm^3 sec^{-1}. If the ambient concentration of NO were 1 ppb, the rate for this reaction is 0.2 sec^{-1}, or a lifetime of 5 sec; this would be a rather clean environment. Typical indoor air NO concentrations (Finlayson-Pitts and Pitts, 2000) range from 5 to 50 ppb, so this reaction probably takes place within 0.1 to 1 sec after the HO_2 is formed. Now most of the hydroperoxyl radicals will still exit the device but will be converted to OH within a centimeter or less as soon as diffusive mixing prevails.

So how does one explain the observed fact (Steinagel 2009; Ramm 2009) that a device such as that described here is able to clean rooms where some of nonvolatile target compound(s)—particularly microorganisms—are far away and cannot be pumped through? This question is especially pertinent concerning mold on surfaces well away from the device; there is no way these will vaporize and pass through the hydroxyl generator. So far as we know, this question has not been previously addressed for any air purifier of this nature.

We posit that this must happen via reactions with the partially oxidized products from the initial OH + hydrocarbon reaction. For compounds with only a few carbon atoms the degradation processes from initial hydrocarbon to H_2O and CO_2 are extremely complex and involve dozens to hundreds of intermediates. Some of these are radicals. One hydrocarbon radical is produced each time a hydroxyl molecule abstracts a hydrogen to form water. In subsequent steps, this hydrocarbon radical rapidly reacts with oxygen to form an oxy or peroxy radical; these species are themselves good oxidizing agents. These intermediates continue to react and form another, different radical— although only one per intial OH—or, eventually, recombine with yet some other radical. The mixture will eventually be stabilized as various oxidation products are formed and the number of radicals diminishes toward zero via the radical recombination. Finlayson-Pitts and Pitts (2000) discuss such mechanisms and illustrate the complexity vividly for the example of the oxidation, initiated by OH, of isoprene, a naturally occurring hydrocarbon for which plants, animals, and humans are sources. A figure depicting "*some major pathways*" (emphasis added) includes 30 partially oxidized hydrocarbons, including acids, alcohols, ketones, and a furan. Of course, when any of these pass through the purifier, they may react further with OH, leading to many more intermediates and the persistence of circulating organic free radicals throughout the treatment environment. (Note that only the reaction paths are shown in that isoprene pathway figure; quantitative information such as branching ratios or reaction rate coefficients is unknown or poorly known for many of these reactions.) If the system runs continuously, some organic compounds will be fully decomposed to yield carbon dioxide and water, but a distribution of various intermediate organic and oxygenated free radicals will always be present.

We presume that such molecules are present in an actual application when a room or some other environment is cleansed by such a hydroxyl generator. At least some, probably many, of these longer lived, partially oxidized but still reactive species will survive long enough to travel around a room, given typical air exchange and flow. They then are the likely candidates for removal of contaminants, such as surface-bound chemicals, microorganisms, and mold, which cannot be transported to the hydroxyl generator itself.

The question then arises, are these radicals present in the room hazardous to individuals? To answer this, it is important to note that the steady-state OH concentration of 3×10^6 molecules/cm^3—averaged throughout the chamber—is very much the same as the steady-state OH concentrations found outdoors during the daytime, which range from 1 to 10×10^6 molecules/cm^3 (Crosley 1995; Stone et al., 2012). In turn, the secondary radicals formed in the reactions initiated by OH must also be at the same concentrations as those found outdoors (recall that only one radical may be formed per initial OH generated). Therefore, none of these radicals pose any danger beyond those found in the natural atmosphere.

This is one way that the radical production rates determined in this study can be used to design safe, effective remediation strategies.

Generation of OH by photolysis of O_3

As noted in the introduction, hydroxyl radicals in the atmosphere are produced by the photolysis of O_3 to generate $O(^1D)$ atoms that react with H_2O vapor, where the photolyzing radiation is at wavelengths above ~315 nm. In our experiment, there is 10-fold the radiation at 254 nm compared to 185 nm, which might photolyze the naturally present O_3; in fact, the photolysis absorption cross section is far higher at 254 than at 315 nm. (In the natural environment, 254-nm radiation from the sun has already been totally absorbed by the stratospheric ozone layer and does not reach the surface of the earth.)

Photolysis of ozone is also the mode of formation of hydroxyl radicals in the method described by Johnson et al. (2014), where O_3 at a few parts per million (produced by an ozone generator that is part of that device) is added to furnish enough of this source gas for sufficient OH production.
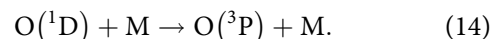
The reactions are:

$$O_3 + h\nu_{254} \rightarrow O_2 + O(^1D); \qquad (12)$$

followed by the reaction:

$$O(^1D) + H_2O \rightarrow 2OH, \qquad (13)$$

or deactiviation:

$$O(^1D) + M \rightarrow O(^3P) + M. \qquad (14)$$

$O(^1D)$ is an electronically excited oxygen atom capable of producing OH by reaction (13); the ground-state $O(^3P)$ cannot form hydroxyls in such a reaction. It does, however, react with an O_2 molecule to reconstitute the ozone, reaction (6).

In a manner similar to that for the OH production rate at 185 nm, we can use this sequence of reactions (Smith and Crosley, 1990), with rate coefficients from DeMore et al. (1997), to calculate the OH production rate at 254 nm. It is convenient to calculate the ratio **R** of the production rates at the two wavelengths, as this is much less

sensitive to the actual value of [H_2O] present. Numerical details are given in the SI. We find that at the background level of 52 ppb ozone, $R = 6.3 \times 10^{-5}$. For even a 10-fold larger concentration, the formation of OH at 254 nm will be negligible compared to that 185 nm, in our experiment.

Modeling the purifier of Johnson et al. (2014)

Johnson et al. (2014; see also Johnson et al.'s supplementary material) recently described a new air-purifying device forming OH entirely via 254-nm photolysis of O_3 with no 185-nm photolysis of H_2O. The goal of this apparatus is somewhat different than that for the purifier investigated in the present paper. The device in this paper is termed "gas phase advanced oxidation," GPAO.

The GPAO aim is full destruction of airborne hydrocarbons by complete oxidation to form secondary organic aerosols; these are removed via electrostatic precipitation, with all the processes occuring within the device. In order to generate sufficient OH, O_3 must be added via an ozone generator near the device inlet, and ozone remaining at the end is removed using a manganese dioxide catalyst.

There are thus two major differences compared with the purifier studied here. First, complete oxidation is accomplished within the device itself, so no volatile organic compounds exit, and thus there is no action outside the device; second, by using O_3 photolysis production, special quartz lamps passing 185 nm are not needed. On the other hand, the second objective requires initial addition of ozone; this together with the first necessitates passage of the entire airflow though filters, limiting the flow velocity and throughput. For example, the device called the "Portable Prototype," which we consider quantitatively in the following, has a volumetric flow of 0.77 m^3/min compared to the device studied here, which was 14 m^3/min. Therefore, one would expect the primary applications of each device to be rather different.

Nevertheless, it is interesting to make a quantitative comparison with the approach used here for our device. We predict the absolute amount of OH generated by O_3 photolysis using the treatment just described, and a loss rate approach similar to our experiment, to predict [OH]$_{ss}$ for the GPAO Portable Prototype. We take numerical values given in Johnson et al. (2014) when available. It was necessary to approximate "a few ppm" given for the O_3 concentration, and "a few milligrams" of added cyclohexane. In each case we use the arbitrary value 3 for "a few."

As before, calculational details are in the SI. We predict in their experimental chamber [OH]$_{ss}$ = 4.4 × 10^6 cm^{-3}.

A kinetics experiment was reported; Figure 8 of Johnson et al. (2014) shows the decays of cyclohexane without the apparatus operating (flow only) and operating (flow plus OH production). The analysis is reported in the supporting information for that study (supplementary material for Johnson et al., 2014). We suspect a numerical error is made there; the correct experimental value for [OH]$_{ss}$ should be (3.79 ± 1.43) × 10^6 cm^{-3}, in excellent agreement with the prediction using the estimate of 3 ppm as the ozone concentration. As for our experiment, this agreement indicates we understand these photolytic processes quite well.

About the authors

David R. Crosley, a chemical physicist, is a private consultant in Palo Alto, CA.

Connie J. Araps is an organic chemist specializing in medicinal, polymer, and photochemistry with Prometheus Strategies, in Delray Beach, FL.

Melanie Doyle-Eisele is an associate research scientist in the Chemistry and Inhalation Exposure Program at Lovelace Respiratory Research Institute in Albuquerque, NM.

Jacob D. McDonald directs the Chemistry and Inhalation Exposure, and Environmental Respiratory Health programs at Lovelace Respiratory Research Institute in Albuquerque, NM.

References

Creasey, D.J., P.A. Halford-Maw, D.E. Heard, M.J. Pilling, and B.J. Whitaker. 1997. Implementation and initial deployment of a field instrument for measurement of OH and HO$_2$ in the troposphere by laser-induced fluorescence. *J. Chem. Soc. Far. Trans.* 93:2907–13. doi:10.1039/A701469D

Creasey, D.J., D.E. Heard, and J.D. Lee. 2000. Absorption cross-section measurements of water-vapour and oxygen at 185 nm. Implications for the calibration of field instruments to measure OH, HO$_2$ and RO$_2$ radicals. *Geophys. Res. Lett.* 27:1651–54. doi:10.1029/1999GL011014

Crosley, D.R. 1995. The measurement of OH in the atmosphere. *J. Atmos. Sci.* 52:3299–314. doi:10.1175/1520-0469 (1995)052<3299:TMOOAH>2.0.CO;2

DeMore, W.B., S.P. Sander, C.J. Howard, A.R. Ravishankara, D.M. Golden, C.E. Kolb, R.F. Hampson, M.J. Kurylo, and M.J. Molina. 1997. *Chemical Kinetics and Photochemical Data for Use in Stratospheric Modelling*. Evaluation 12, JPL Publication 97-4. Pasadena, CA: NASA Jet Propulsion Laboratory.

Finlayson-Pitts, B.J., and J.N. Pitts, Jr. 2000. *Chemistry of the Upper and Lower Atmosphere*. San Diego, CA: Academic Press.

Johnson, M.S., E.J.K. Nilsson, E.A. Svensson, and S. Langer. 2014. Gas-phase advanced oxidation for effective, efficient in situ control of pollution. *Environ. Sci. Technol.* 48:8768–76. doi:10.1021/es5012687

Logan, J.A., M.J. Prather, S.C. Wofsy, and M.E. McElroy. 1981. Tropospheric chemistry: A global perspective. *J. Geophys. Res.* 86:7210–54. doi:10.1029/JC086iC08p07210

Mo, J., Y. Zhang, Q. Xu, J.L. Lamson, and R. Zhao. 2009. Photocatalytic purification of volatile organic compounds in indoor air: A literature review. *Atmos. Environ.* 43:2229–46. doi:10.1016/j.atmosenv.2009.01.034

Morneault, G.J.E. 2010. Hydroxyl generator. U.S. Patent 2010/0272600A1.

Ramm, K.H. 2009. Evaluation of antiviral activity of uv illumination/hydroxyl generator, ATS Laboratories Reports, available at hgiind.com/hydroxyls, under Lab Results.

Smith, G.P., and D.R. Crosley. 1990. A photochemical model of ozone interference effects in laser detection of tropospheric OH. *J. Geophys. Res.* 90:16427–42. doi:10.1029/JD095iD10p16427

Steinagel, S. 2009. Evaluation of microbial activity of uv illumination/hydroxyl generator. ATS Laboratories Reports. hgiind.com/hydroxyls, under Lab Results.

Stone, D., L.K. Whalley, and D.E. Heard. 2012. Tropospheric OH and HO_2 radicals: Field measurements and model comparisons. *Chem. Soc. Rev.* 41:6348–404. doi:10.1039/C2CS35140D

Weatherspark. 2015. https://weatherspark.com/averages/29581/Albuquerque-New-Mexico-United-States (accessed February 2015).

Weschler, C.J. 2009. Changes in indoor air pollutants since the 1950s. *Atmos. Environ.* 43:153–69. doi:10.1016/j.atmosenv.2008.09.044

Weschler, C.J., and H.C. Shields. 1996. Production of the hydroxyl radical in indoor air. *Environ. Sci. Technol.* 30:3250–58. doi:10.1021/es960032f

Yoshino, K., D.R.E. Freeman, and W.H. Parkinson. 1984. Atlas of the Schumann–Runge absorption bands of O_2 in the wavelength region 175–205 nm. *J. Chem. Phys. Ref. Data* 13:207–27. doi:10.1063/1.555702